PROCEEDINGS OF SPIE

SPIEDigitalLibrary.org/conference-proceedings-of-spie

Reliability estimation of armchair-based capacitive ECG using video-based pose estimation

Satyam Srivastava, Arman Ershadi, Mostafa Haghi, Thomas Deserno

Satyam Srivastava, Arman Ershadi, Mostafa Haghi, Thomas M. Deserno, "Reliability estimation of armchair-based capacitive ECG using video-based pose estimation," Proc. SPIE 12469, Medical Imaging 2023: Imaging Informatics for Healthcare, Research, and Applications, 124690E (10 April 2023); doi: 10.1117/12.2654327

SPIE.

Event: SPIE Medical Imaging, 2023, San Diego, California, United States

Reliability estimation of armchair-based capacitive ECG using video-based pose estimation

Satyam Srivastava[a], Arman Ershadi[b], Mostafa Haghi[b], and Thomas M. Deserno[b]

[a]Birla Institute of Technology & Science, Pilani, India
[b]Peter L. Reichertz Institute for Medical Informatics of TU Braunschweig and Hannover Medical School, Braunschweig, Germany

ABSTRACT

Background: Annually and globally, cardiovascular diseases yield the death of 17.9 million people. Continuous and unobtrusive monitoring of vital signs supports an early detection of abnormalities and diseases, such as atrial fibrillation. Here, we analyze capacitive electrocardiography (cECG) recorded in an armchair at home. However, processing such data is challenging, as body movements and other artifacts disturb the signal quality. Methods: In this paper, we suggest video-based pose estimation to assess the reliability of cEGC. In 20 subjects, we measured reference and capacitive ECG synchronized with a video recording for key-point-based movement analysis with the OpenPifPaf pose estimation algorithm. We considered all 17 human body joints to compute a movement index and label all data in windows of 5 s as reliable vs. unreliable, according to that index. Then, we compared the heart rates obtained from complete and reliable cEGC windows with the corresponding windows from the reference ground truth ECG. Result: The left and right hip joints are most significantly influencing the signal's quality. In addition, the joints' movement distance from the original position limited to the range 460.84 pixels and 382.22 pixels, respectively, deliver a reliable cECG signal. Conclusion: Video-based pose estimation delivers reliable and unreliable periods of cECG recordings and improves continuous health monitoring at home.

Keywords: Signal processing, ECG signal analysis, Pose estimation, Neural network, In-home monitoring.

1. INTRODUCTION

Cardiovascular diseases (CVD) accounted for 32% of all global deaths in 2019, World Health Organization (WHO) reported.[1] Of these, 8% were caused due to heart attack and stroke. CVDs caused 38% of the 17 million premature deaths under the age of 70 due to non-communicable diseases in 2019.[1,2] Adequate care of diet, physical activity, and control of alcohol consumption and tobacco use can prevent most CVDs.[2]

With the increasing cases of CVDs worldwide, from one side[1] and improving the methods, techniques, and technology of continuous and unobtrusive in-home monitoring,[2] from the other side, it is necessary and possible to detect these diseases in the early stages in order to deliver an efficient treatment to the patient.[3] Capacitive electrocardiography (cECG) measures the bio-potential differences, enabling non-contact patient monitoring.[4]

The capacitively coupled electrodes measure the activity of the heart muscles by measuring the electric potential from the body surface, even from above the layers of clothing.[3,4] The application of the cECG electrodes has been reported for the continuous and unobtrusive monitoring of the heart rate (HR), in the private spaces such as vehicle[5,6] and home,[7,8] embedded in beds and chairs.[9]

However, the cECG signal suffers from various factors such as movements and artifacts,[10] coupling impedance,[11] and electromagnetic interference (EMI),[12,13] which disrupt the signal quality and decrease the signal-to-noise ratio (SNR) and its reliability for measuring the cardiac parameters. The voluntary/involuntary movements of the human body can affect the ECG signal and hence creating uncertainty on the signal reliability.
The signal quality assessment (SQA) plays a pivotal role in overcoming the problem and improving the SNR. The exact determination of ECG signal characteristic points is important for detecting CVDs and other applications of ECG signals.[13]

Further author information: (Send correspondence to M.H.)
M.H.: E-mail: mostafa.haghi@htwg-konstanz.de

Medical Imaging 2023: Imaging Informatics for Healthcare, Research, and Applications,
edited by Brian J. Park, Hiroyuki Yoshida, Proc. of SPIE Vol. 12469, 124690E
 · 1605-7422 · doi: 10.1117/12.2654327

Satija et al. have grouped the various methods for SQA of clinical ECG into five categories: (i) fiducial features and heuristic rules-based SQA methods, (ii) fiducial features and machine learning-based SQA methods, (iii) nonfiducial features and heuristic rules based SQA methods, (iv) nonfiducial features and machine learning based SQA methods, (v) filtering-based SQA methods.[13] Hou et al. developed an SQA approach for cECG signals based on the phase-space reconstruction.[9] Wartzek et al. proposed that contact electrification and triboelectricity as the reasons for artifacts in the cECG signal and worked on developing different electrode designs to minimize the effect.[12] Fukuyama et al. investigated multi-layered fabric electrodes with the non-layered ones in terms of movement artifact reduction.[14]

However, the SQA based on the key-joints' movement data from the subject has not been explored yet. In this study, we have proposed the neural network-based approach to classify the cECG signal based on its reliability from the key-joints-based movement data collected from the subject using the pose estimation algorithm. We use the signal from the adhesive Plux sensors (ECG Plux sensor, Plux, Lisbon, Portugal) as the reference for classifying the cECG signal and, therefore, towards the model's learning.

2. MATERIALS AND METHODS

We propose a novel pipeline for the cECG signal classification based on extracting the key-point based movements of human body from the video recording (Figure 1). We used 11 minutes of video recordings of 20 subjects sitting on the cECG armchair while reading books and turning over the pages (Figure 2). We conducted the recordings under similar circumstances, e.g., temperature and humidity; none of the subjects declared any known CVDs, while all subjects filled and signed the consent form. We recorded the ECG ground truth and cECG (Capical GmbH, Braunschweig, Germany) in 500 Hz and 560 Hz, respectibely. Besides, we recorded the key-point coordinates using the pose estimation at 10 frames per second (FPS).

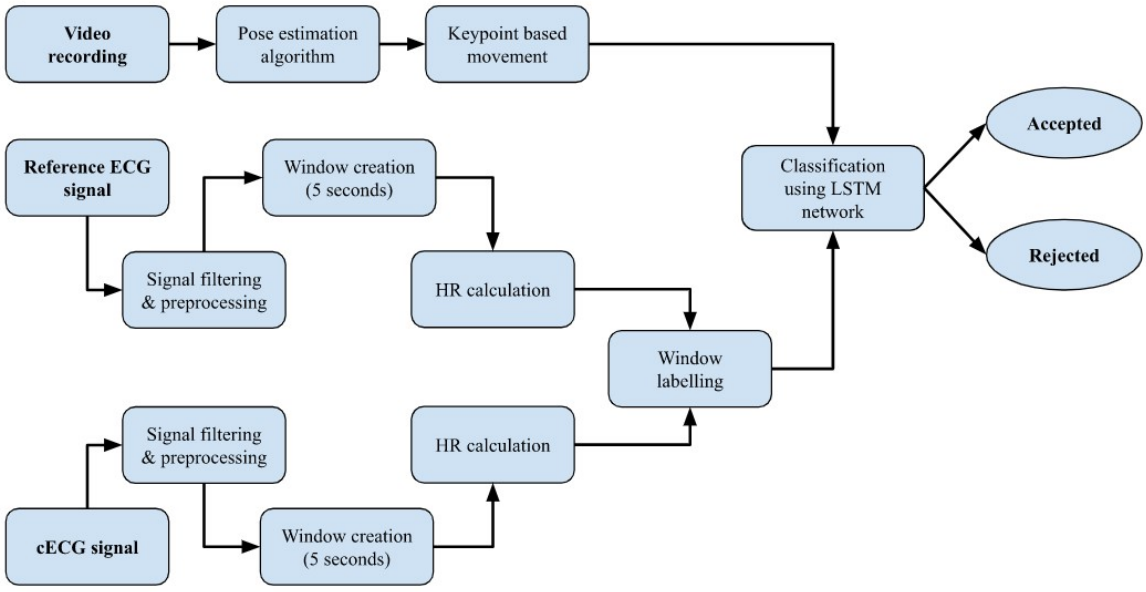

Figure 1. An overview of our proposed pipeline for the cECG classification

The Plux and cECG sensors were time synchronized using an optical synchronization interface. The video recording of joints and pose estimation was then synchronized with the signal by calculating the offset timestamp individually customized for each subject. The signals were filtered using the bandpass filter with the standard range of 0.05 Hz and 100 Hz as the low and high cut-off frequencies, respectively.

We divided the ECG signals into windows of 5 seconds[15] to calculate HR from both the Plux and Capical sensors using the HeartPy module.[16] The HeartPy module computes the HR as the average beat-beat interval

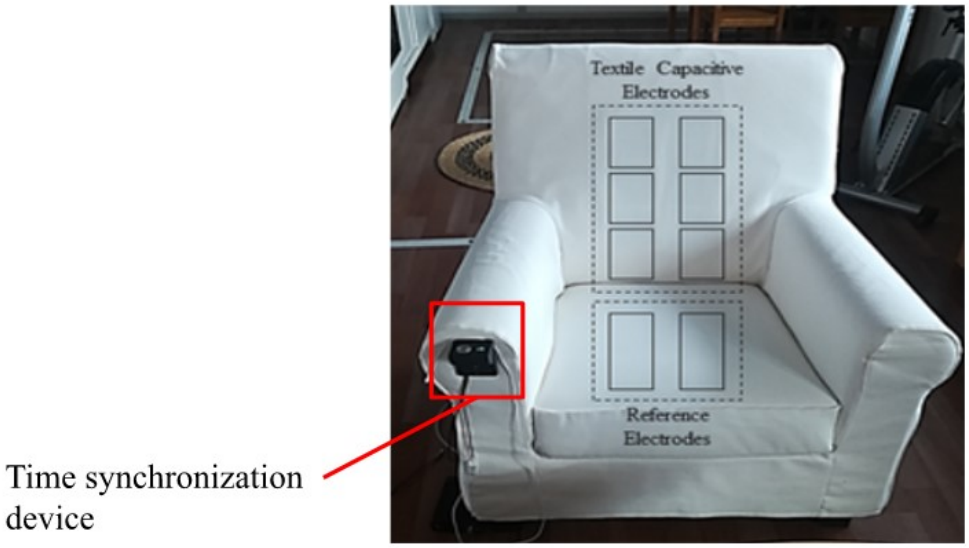

Figure 2. Representative position of capacitive electrodes in cECG armchair

across the entire analyzed signal. To check upon the accuracy of the peaks and reject the false peaks, it measures the HR variability using the root mean square of the successive differences (RMSSD). Figure 3 shows the representative signal and RMSSD calculated using the equation 1:

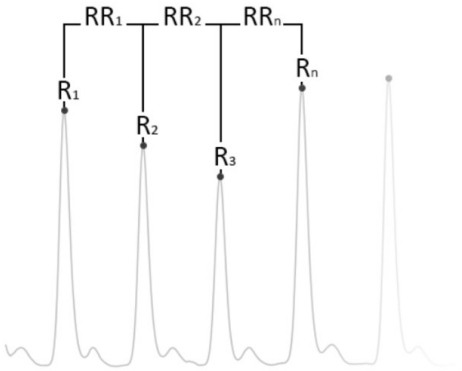

Figure 3. Representative signal image. Source: HeartPy documentation[16]

$$RMSSD = \sqrt{\frac{1}{n-2}\sum_{i=0}^{n-2}(RR_i - RR_{i+1})^2} \tag{1}$$

RMSSD is calculated on the basis of the number of R-peaks denoted by 'n', RR_i denoted the R interval from the i_{th} peak, whereas the RR_{i+1} denotes the R interval from the $i+1_{th}$ peak. The summation of the square of each of the succesive time difference is then averaged to calculate the RMSSD. Having HR from the Plux sensor as the reference, the window of the cECG was either marked as accepted (reliable signal) or rejected (unreliable signal). If the calculated HR of cECG was in the 90% range of HR from the Plux, the reliability criteria was met.[17]

The calculated HR from reference and cECG in the window of 5 seconds is as shown in Figure 4 for one of the subject. The gaps of HR from cECG represent the unreliable regions of the signal.

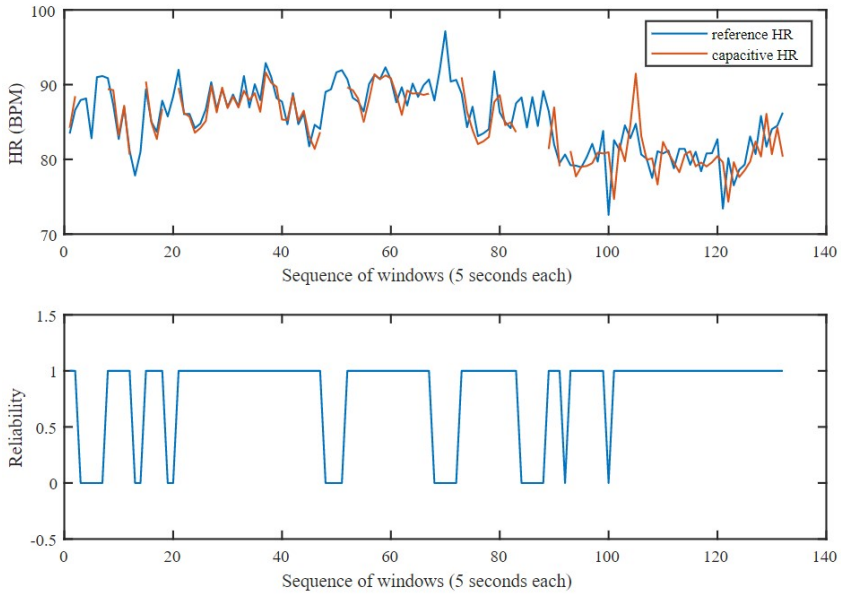

Figure 4. HR calculated from Plux and cECG are compared for identifying the reliable and unreliable regions

Labeling accepted and rejected windows (see Figure 5 and Figure 6) is based on the HR criteria computed from the Plux ECG.

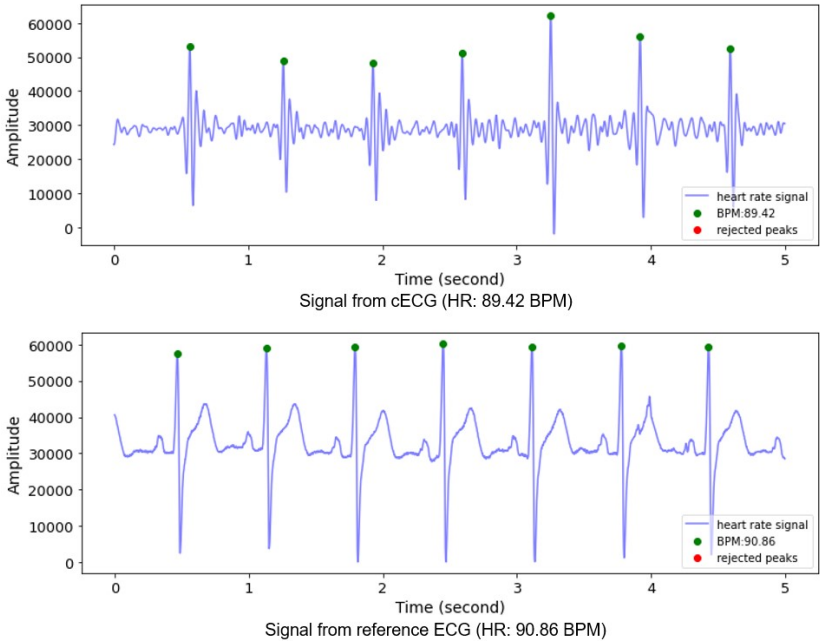

Figure 5. Accepted Window (labelled as '1') as the HR calculated from the cECG signal lie in the 90% range of the HR from the reference ECG

The movement of the human body was calculated with the key point-based method. We used pose estimation

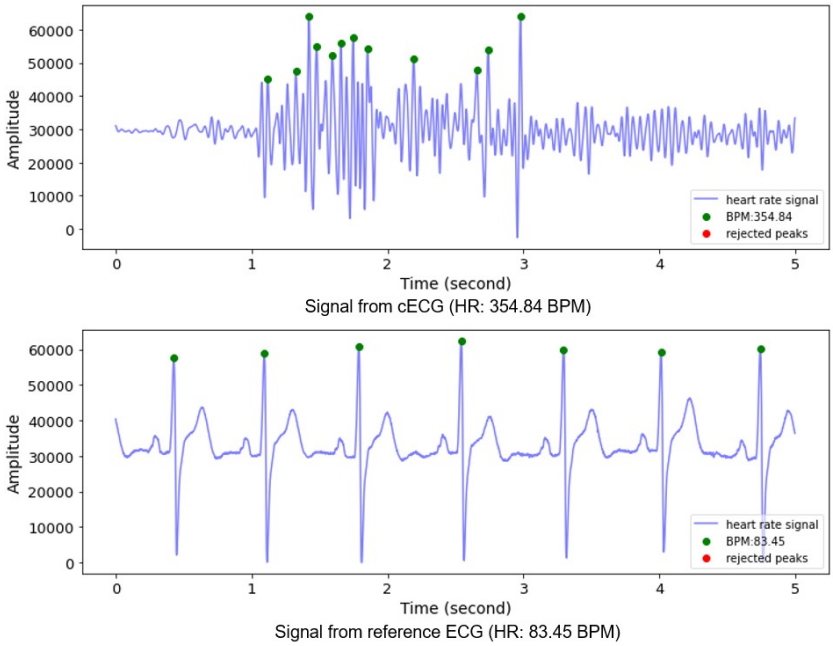

Figure 6. Rejected Window (labelled as '0') as the HR calculated from the cECG signal does not lie in the 90% range of the HR from the reference ECG

algorithm OpenPifPaf[18] to record the coordinates from the 17 major joints of the human body (see Figure 7) every 100 ms.
Based on these coordinates, the absolute distance moved by each joint was calculated using the equation 2:

$$d(A, B) = \sqrt{(x - x') + (y - y')} \tag{2}$$

The *d(A,B)* defines the distance between the two points denoted by A and B with the 2-d coordinates as *(x, y)* and *(x', y')*.

Figure 7. Representative image of 17 human body joints. Source: COCO 2017 dataset[18]

The movements data and the cECG window labels (accepted: '1' and rejected: '0'), were fed to the neural network for training and testing the model performance. The visual representation of the movement data in

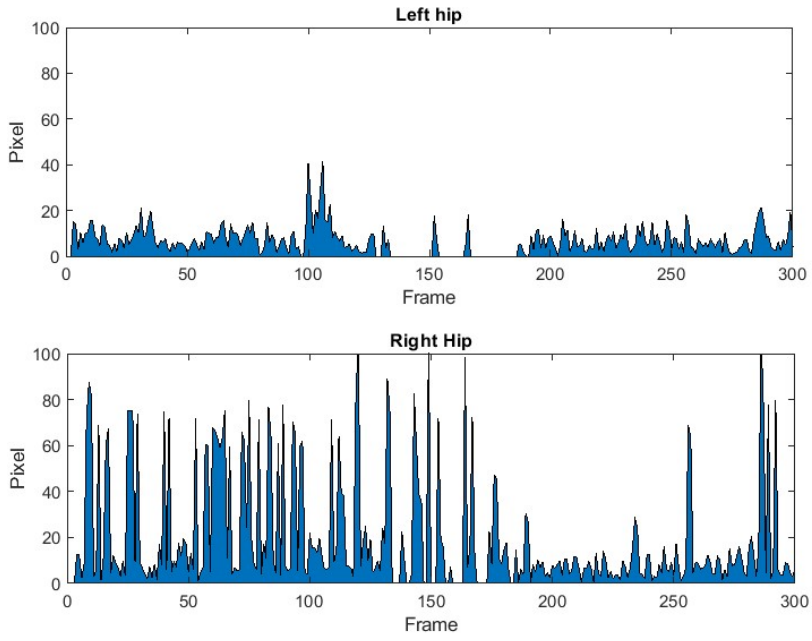

Figure 8. Movement data from significant joints

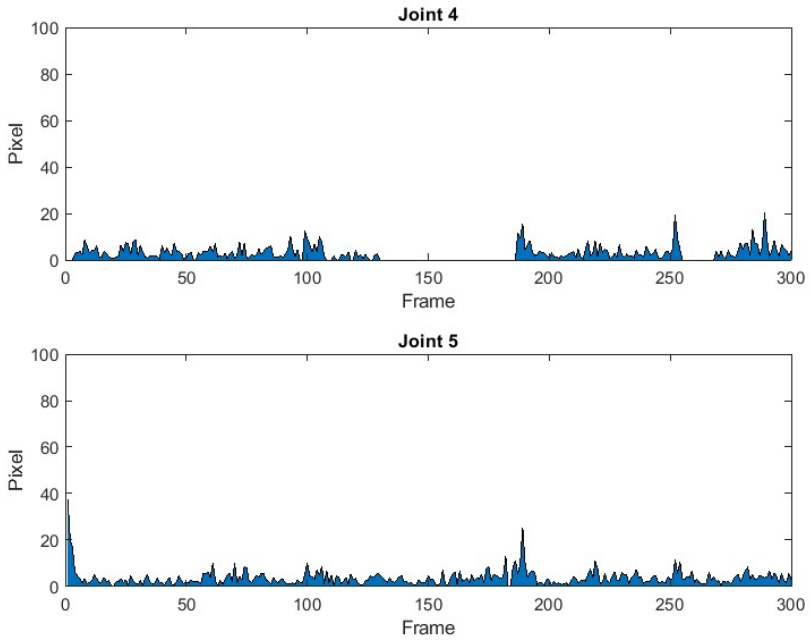

Figure 9. Movement data from less significant joints

pixels for the 30 seconds of time period for both the significant and the less significant joints are shown as in Figure 8 and Figure 9 respectively. The left and right hip were found to be the significant ones in our study.

The movement data for the same 30 seconds of window for the combined sum of movement from all the 17 joints is as shown in Figure 10.

We developed a long short term memory (LSTM) neural network, which is well suited to the classification

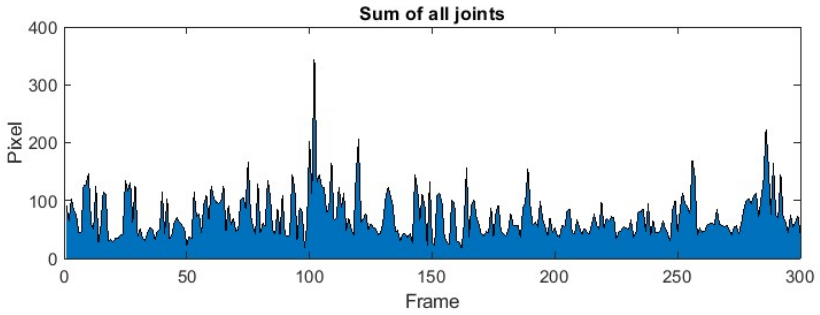

Figure 10. Movement data from the summation of all the 17 joints of a subject

problems of time series sequential data.[19,20] It is a special kind of recurrent neural network (RNN), capable of handling the problem of vanishing gradient which is encountered while training the traditional RNNs. The developed LSTM consists of a single input layer connected to 100 LSTM cells along with hidden states. The output of the LSTM layer is then passed on to the fully connected layer which transforms the hidden states into two classes of classification (see Figure 11).

Having the total accepted and rejected windows of 82% and 18% respectively, caused an imbalance in the whole dataset. we observedthe model tendency towards false positive classification. IThus, we applied the approach of synthetic data generation[21] using the Gaussian noise. After feeding the movement data of 17 joints obtained from 20 subjects, along with the signal classification and synthetic data generation, to the neural network, we trained the model for ten rounds, each comprising 100 epochs. We used the random data split in the ratio of 80:20 for our training set and testing set, respectively.

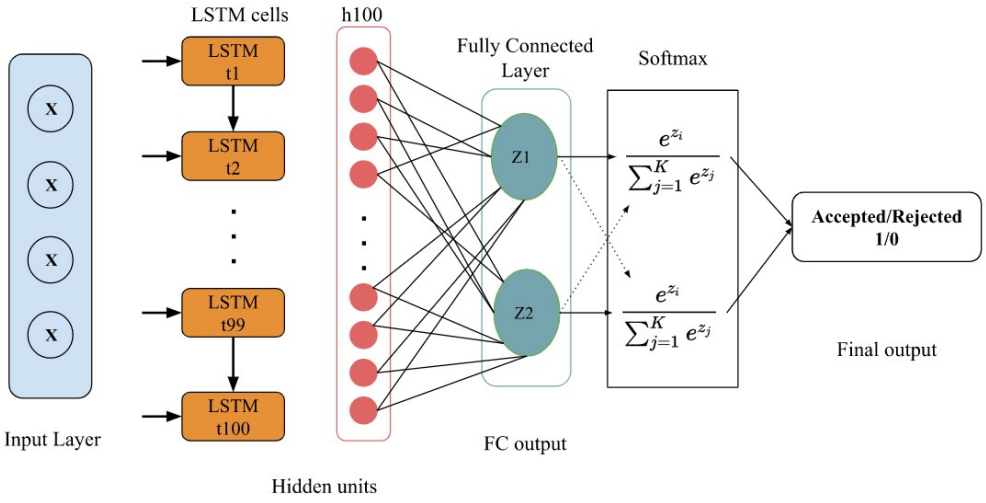

Figure 11. LSTM Neural Network Architecture

3. RESULTS

The mean confusion matrix is shown in Figure 12. The confusion matrix provides insight into the performance of the classification algorithm by providing the error in the results from the predicted and actual label classes. The four basic characteristics of the confusion matrix used to define the measurement metrics of the classifier and our results are as follows:

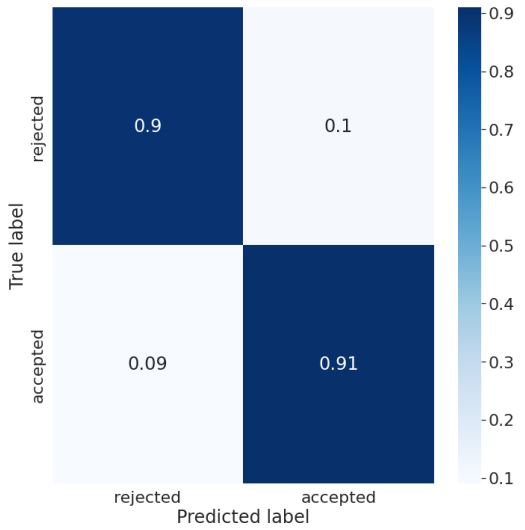

Figure 12. Mean confusion matrix for evaluating the performance of classification model (after 10 rounds)

- TP (True Positive): % of windows that have been correctly classified as accepted of the total accepted windows - 91%
- TN (True Negative): % of windows that have been correctly classified as rejected of the total rejected windows - 90%
- FP (False Positive): % of windows that have been misclassified as accepted of the total rejected windows - 10%
- FN (False Negative): % of windows that have been misclassified as rejected of the total accepted windows - 09%

The mean F1 score was 90.48%. Using the LSTM feature importance, we obtained the significance of each joint along with that of the summation of all joints (represented by "sum" in the figure) on the model's performance (see Figure 13). Our results showed that the movement originated from the left and right hip joints were the most significant joints on the signal reliability. For each feature that we conducted the evaluation, we shuffled the feature column randomly and calculate the mean absolute error (MAE).

If a feature has a significant impact on the LSTM model, then the MAE became worse with that feature permuted. We went through this procedure for all the features. Figure 13 indicates that how worse MAE is without each feature, which is the importance of each feature.
We found the maximum movement for the most effective joints, at which the quality of signal and the reliability of the window are still maintained. The left and right hips were found to be 460.84 pixels and 382.22 pixels, respectively.

4. DISCUSSION

One of the popular and feasible methods of continuous health monitoring for the early detection of CVDs is through non-contact/ non-invasive measurement. The existing signal processing and analysis from the cECG electrodes mostly focused on the disturbances from the human body movement and artifact and do not correlate the motion and signal, which can be seen as an instruction to the user to use such technology for reliable and usable monitoring. This will help to improve the existing state-of-the-art cECG signal quality.[10,17,22,23]

Our study was, however, limited to 11 minutes of data recording from 20 subjects, all of them being free from any chronic heart complications. The subjects were assigned the task of reading, which might not take into

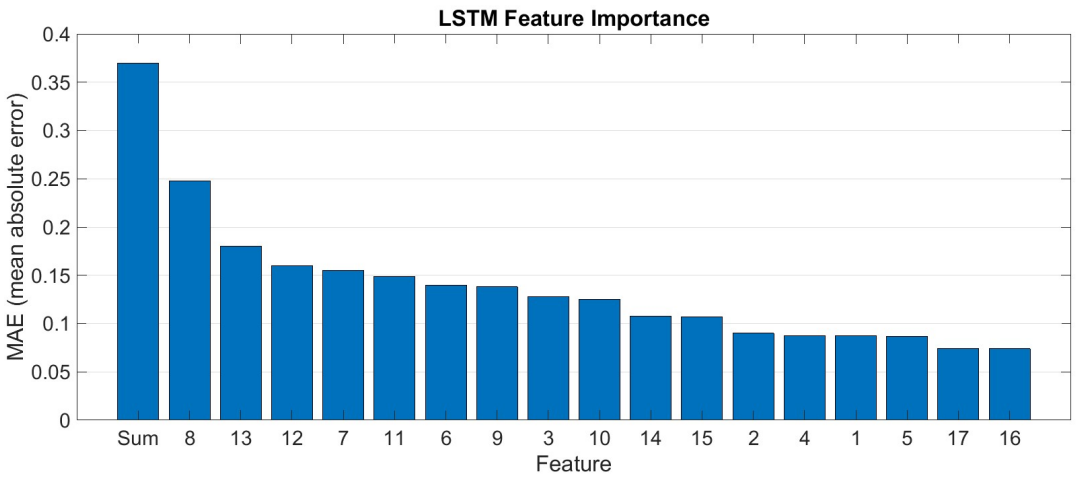

Figure 13. Relative importance of each joint.

account all the types of body movements, leading to only partial learning of the neural network. In addition, the application of this method for data recording during daily living could give a better perspective, which is the subject of our next study.

The model was also trained with the data in the smart home lab environment and not the actual living home environment.

While estimating the importance of the joint from the feature importance, we also found the left elbow as the most significant joint. However, we expect the same should be reflected in the output with respect to the right elbow, and this is the consequence of an imbalanced dataset and limited types of activity (the majority of subjects turn over the book with their left hand). This could be because of the more movements from that joint in the specific activity of reading. Movement from all the 17 human body joints were treated equally for the classification of the cECG signal reliability. Based on the literature research and from the knowledge of medical science, not all the joint movement have equal affect on the signal quality. Since, some of the joints have more effect than the others, a weighted sum approach could give better results and robust algorithm for our classification algorithm.

5. CONCLUSION

From this study, we can conclude that different joints of the body can have drastic effects on the cECG signal and HR measurement. Some joints at the central part of the body such as the left and right hip, contribute significantly and have more importance. The study shows that even though movement can cause disruption to the signal; it depends on the type of activity and the certain degree of joint movement associated with it. Considering a limited movement within the allowed range still can contribute to a reliable ECG signal, leading to an effective, unobtrusive monitoring.

REFERENCES

[1] Cardiovascular diseases (CVDs) [Internet]. World Health Organization. World Health Organization; [cited 2022Sep10];. Available from: https://www.who.int/en/news-room/fact-sheets/detail/cardiovascular-diseases-(cvds).

[2] Timmis A, Vardas P, Townsend N, Torbica A, Katus H, De Smedt D, et al. European Society of Cardiology: cardiovascular disease statistics 2021. European Heart Journal. 2022;43(8):716-99.

[3] Gao Y, Soman VV, Lombardi JP, Rajbhandari PP, Dhakal TP, Wilson DG, et al. Heart monitor using flexible capacitive ECG electrodes. IEEE Transactions on Instrumentation and Measurement. 2019;69(7):4314-23.

[4] Sun Y, Yu XB. Capacitive biopotential measurement for electrophysiological signal acquisition: A review. IEEE Sensors Journal. 2016;16(9):2832-53.

[5] Wang J, Spicher N, Warnecke JM, Haghi M, Schwartze J, Deserno TM. Unobtrusive health monitoring in private spaces: The smart home. Sensors. 2021;21(3):864.
[6] Wartzek T, Eilebrecht B, Lem J, Lindner HJ, Leonhardt S, Walter M. ECG on the road: Robust and unobtrusive estimation of heart rate. IEEE Transactions on biomedical engineering. 2011;58(11):3112-20.
[7] Castro ID, Patel A, Torfs T, Puers R, Van Hoof C. Capacitive multi-electrode array with real-time electrode selection for unobtrusive ECG & BIOZ monitoring. In: 2019 41st Annual International Conference of the IEEE Engineering in Medicine and Biology Society (EMBC). IEEE; 2019. p. 5621-4.
[8] Kido K, Tamura T, Ono N, Altaf-Ul-Amin M, Sekine M, Kanaya S, et al. A novel CNN-based framework for classification of signal quality and sleep position from a capacitive ECG measurement. Sensors. 2019;19(7):1731.
[9] Hou Z, Xiang J, Dong Y, Xue X, Xiong H, Yang B. Capturing electrocardiogram signals from chairs by multiple capacitively coupled unipolar electrodes. Sensors. 2018;18(9):2835.
[10] Lee JS, Heo J, Lee WK, Lim YG, Kim YH, Park KS. Flexible capacitive electrodes for minimizing motion artifacts in ambulatory electrocardiograms. Sensors. 2014;14(8):14732-43.
[11] Eilebrecht B, Willkomm J, Pohl A, Wartzek T, Leonhardt S. Impedance measurement system for determination of capacitive electrode coupling. IEEE Transactions on Biomedical Circuits and Systems. 2013;7(5):682-9.
[12] Wartzek T, Lammersen T, Eilebrecht B, Walter M, Leonhardt S. Triboelectricity in capacitive biopotential measurements. IEEE Transactions on Biomedical Engineering. 2010;58(5):1268-77.
[13] Satija U, Ramkumar B, Manikandan MS. A review of signal processing techniques for electrocardiogram signal quality assessment. IEEE reviews in biomedical engineering. 2018;11:36-52.
[14] Fukuyama Y, Suzuki R, Takayama S, Ueno A. Multi-layered fabric electrode for movement artifact reduction in capacitive ECG measurement. In: 2013 35th Annual International Conference of the IEEE Engineering in Medicine and Biology Society (EMBC). IEEE; 2013. p. 555-8.
[15] Tanantong T. A study on the effects of window size on electrocardiogram signal quality classification. 2016.
[16] Van Gent P, Farah H, Van Nes N, Van Arem B. HeartPy: A novel heart rate algorithm for the analysis of noisy signals. Transportation research part F: traffic psychology and behaviour. 2019;66:368-78.
[17] Warnecke JM, Wang J, Cakir T, Spicher N, Ganapathy N, Deserno TM. Registered report protocol: Developing an artifact index for capacitive electrocardiography signals acquired with an armchair. Plos one. 2021;16(7):e0254780.
[18] Kreiss S, Bertoni L, Alahi A. Openpifpaf: Composite fields for semantic keypoint detection and spatio-temporal association. IEEE Transactions on Intelligent Transportation Systems. 2021.
[19] Breuel TM. Benchmarking of LSTM networks. arXiv preprint arXiv:150802774. 2015.
[20] Yu Y, Si X, Hu C, Zhang J. A review of recurrent neural networks: LSTM cells and network architectures. Neural computation. 2019;31(7):1235-70.
[21] Dahmen J, Cook D. SynSys: A synthetic data generation system for healthcare applications. Sensors. 2019;19(5):1181.
[22] Xu L, Rabotti C, Zhang Y, Ouzounov S, Harpe PJ, Mischi M. Motion-artifact reduction in capacitive heart-rate measurements by adaptive filtering. IEEE Transactions on Instrumentation and Measurement. 2018;68(10):4085-93.
[23] Serteyn A, Vullings R, Meftah M, Bergmans JW. Motion artifacts in capacitive ECG measurements: Reducing the combined effect of DC voltages and capacitance changes using an injection signal. IEEE Transactions on Biomedical Engineering. 2014;62(1):264-73.